Mutations within the membrane domain of HMG-CoA reductase confer resistance to sterol-accelerated degradation

Peter C. W. Lee, Andrew D. Nguyen, and Russell A. DeBose-Boyd[1]

Department of Molecular Genetics, University of Texas Southwestern Medical Center, Dallas, TX 75390-9046

Abstract **The pivotal event for sterol-induced degradation of the cholesterol biosynthetic enzyme HMG-CoA reductase is binding of its membrane domain to Insig proteins in the endoplasmic reticulum. Insigs are carriers for gp78, an E3 ubiquitin ligase that marks reductase for proteasomal degradation. We report here the isolation of mutant Chinese hamster ovary cell lines, designated SRD-16, -17, and -18, in which sterol-induced ubiquitination and degradation of reductase are severely impaired. These cells were produced by chemical mutagenesis and selection with SR-12813, a compound that mimics sterols in stimulating ubiquitination and degradation of reductase. Each SRD cell line was found to contain a point mutation in one reductase allele, resulting in substitutions of aspartate for serine-60 (SRD-16), arginine for glycine-87 (SRD-17), and proline for alanine-333 (SRD-18). Sterols failed to promote ubiquitination and degradation of these reductase mutants, owing to their decreased affinity for Insigs. Thus, three different point mutations in reductase, all of which localize to the membrane domain, disrupt Insig binding and abolish sterol-accelerated degradation of the enzyme.**—Lee, P. C. W., A. D. Nguyen, and R. A. DeBose-Boyd. **Mutations within the membrane domain of HMG-CoA reductase confer resistance to sterol-accelerated degradation.** ***J. Lipid Res.*** **2007.** 48: **318–327.**

Supplementary key words cholesterol homeostasis • endoplasmic reticulum-associated degradation • ubiquitination • somatic cell genetics • mutagenesis • membrane attachment region • 3-hydroxy-3-methylglutaryl coenzyme A reductase

The enzyme HMG-CoA reductase catalyzes the two-step reduction of HMG-CoA to mevalonate, a rate-determining reaction in the synthesis of cholesterol and nonsterol isoprenoids (1). HMG-CoA reductase, a resident glycoprotein of the endoplasmic reticulum (ER), is integrated into membranes through a hydrophobic NH_2-terminal domain that contains eight membrane-spanning segments separated by short loops (2). The membrane domain of reductase precedes a hydrophilic COOH-terminal domain that projects into the cytosol and contains all enzymatic activity (3, 4). Sterol and nonsterol end products of mevalonate metabolism exert stringent feedback control on reductase through multiple mechanisms, one of which involves accelerated degradation of the enzyme (5–7). The central event in this degradation is the sterol-induced binding of reductase to ER membrane proteins called Insig-1 and Insig-2 (8, 9). Formation of the reductase-Insig complex is mediated by the membrane domain of reductase and results in the recruitment of gp78, a membrane-bound ubiquitin ligase that catalyzes reductase ubiquitination (10). This sterol-induced ubiquitination is an obligatory reaction for the proteasome-mediated degradation of reductase (11).

Insigs play a substantial role in another mechanism for the feedback regulation of reductase by modulating the activity of sterol-regulatory element binding protein (SREBP) cleavage-activating protein (SCAP) (12). Like reductase, SCAP is embedded in ER membranes through a hydrophobic NH_2-terminal domain with eight membrane-spanning segments. The COOH-terminal domain of SCAP projects into the cytosol and mediates complex formation with the SREBP family of transcription factors (13, 14). In sterol-deprived cells, SCAP facilitates the translocation of membrane-bound SREBPs from the ER to the Golgi, where the NH_2-terminal transcription factor domain of SREBPs is proteolytically released into the cytosol. From the cytosol, processed SREBPs rapidly migrate into the nucleus to enhance the transcription of genes encoding reductase and other cholesterol biosynthetic enzymes (15–18). When cells are treated with cholesterol or oxysterols such as 25-hydroxycholesterol (25-HC), SCAP-SREBP complexes are trapped in the ER and SREBP processing is abolished; rates of SREBP target gene transcription and cholesterol syn-

Manuscript received 1 November 2006.

Published, JLR Papers in Press, November 7, 2006.
DOI 10.1194/jlr.M600476-JLR200

Abbreviations: CHO, Chinese hamster ovary; CMV, cytomegalovirus; EMS, ethylmethane sulfonate; ER, endoplasmic reticulum; 25-HC, 25-hydroxycholesterol; LPDS, lipoprotein-deficient serum; SCAP, sterol-regulatory element binding protein cleavage-activating protein; SREBP, sterol-regulatory element binding protein.

[1] To whom correspondence should be addressed.
e-mail: russell.debose-boyd@utsouthwestern.edu

thesis decline (19). The block in ER-to-Golgi transport occurs through sterol-induced binding of SCAP to Insigs (20, 21). This binding is mediated by a segment of ~170 amino acids in SCAP that constitute transmembrane helices 2–6, which resemble the corresponding region in reductase (22). This region is known as the sterol-sensing domain (23, 24). Point mutations within the sterol-sensing domains of SCAP and reductase prevent their association with Insigs, thereby abolishing the sterol-mediated ER retention of SCAP-SREBP complexes and the sterol-induced ubiquitination/degradation of reductase (8, 20, 21, 25, 26).

In the course of dissecting the mechanism for the sterol-accelerated degradation of reductase, we embarked upon a genetic analysis of the process in Chinese hamster ovary (CHO) cells using the 1,1-bisphosphonate ester SR-12813 (27). In cultured cells, SR-12813 limits cholesterol synthesis by stimulating Insig-dependent ubiquitination and degradation of reductase, but the drug does not promote ER retention of SCAP-SREBP. Culture of normal cells in the presence of lipoprotein-deficient serum (LPDS) renders cells entirely dependent on endogenous cholesterol synthesis for survival. Under these conditions, addition of SR-12813 kills cells by triggering the degradation of reductase, thus abrogating cholesterol synthesis. This killing forms the basis for the selection of mutant cells defective in accelerating reductase degradation. Our initial mutagenesis experiments yielded SRD-14 cells, which harbor a partial deletion of the *INSIG-1* gene that leads to deficiencies in Insig-1 mRNA and protein (27). As a result of their Insig-1 deficiency, SRD-14 cells fail to accelerate reductase degradation in the presence of sterols or SR-12813 and the rate of sterol-mediated suppression of SREBP processing in the cells is blunted.

Owing to the specificity of SR-12813 in accelerating reductase degradation, it should be possible to use the drug to isolate mutant cells that have specific defects in reductase degradation but normal regulation of SREBP processing. This study describes the characterization of three mutant SR-12813-resistant CHO cell lines, in which reductase is resistant to ubiquitination and degradation mediated not only by SR-12813 but by sterols as well. In contrast, the mutant cells retain their sensitivity to the sterol-mediated suppression of SREBP processing. In all three mutant cell lines, resistance was traced to point mutations within the membrane domain of reductase that resulted in substitutions of aspartate (Asp) for serine-60 (Ser-60), arginine (Arg) for glycine-87 (Gly-87), and proline (Pro) for alanine-333 (Ala-333). Overexpression of the S60N, G87R, or A333P versions of reductase conferred the resistance of wild-type cells to chronic culture in SR-12813, demonstrating the dominant nature of each mutation. Moreover, all three mutant forms of reductase were refractory to sterol-mediated ubiquitination and degradation, owing to decreased affinity for Insigs. These results highlight the importance of interactions between Insigs and the membrane domain of reductase in the feedback control of a rate-determining step in cholesterol synthesis.

MATERIALS AND METHODS

Materials

We obtained MG-132 and digitonin from Calbiochem; horseradish peroxidase-conjugated donkey anti-mouse and anti-rabbit IgGs (affinity-purified) from Jackson ImmunoResearch Laboratories; ethylmethane sulfonate (EMS) was from Sigma; hydroxypropyl-β-cyclodextrin was from Cyclodextrin Technologies Development; and sterols (25-HC, lanosterol, and cholesterol) were from Steraloids, Inc. (Newport, RI). SR-12813 was synthesized by the Core Medicinal Chemistry Laboratory, Department of Biochemistry, University of Texas Southwestern Medical Center. LPDS ($d > 1.215$ g/ml) was prepared from newborn calf serum by ultracentrifugation (28). Other reagents were obtained from sources described previously (16).

Cell culture

CHO-7 cells were maintained in medium A (1:1 mixture of Ham's F-12 medium and Dulbecco's modified Eagle's medium containing 100 U/ml penicillin and 100 μg/ml streptomycin sulfate) supplemented with 5% (v/v) LPDS. CHO-7/pInsig-2 cells were generated by the stable transfection of CHO-7 cells with pCMV-Insig-2-Myc, an expression plasmid encoding human Insig-2 followed by six copies of the c-Myc epitope (29). CHO-7/pInsig-2 and SRD-13A cells, mutant CHO cells lacking SCAP (30), were maintained in medium A supplemented with 5% fetal calf serum, 1 mM mevalonate, 20 μM sodium oleate, 5 μg/ml cholesterol, and 500 μg/ml G418. All of the cells were grown in a monolayer at 37°C in an 8–9% CO_2 incubator.

Mutagenesis and isolation of SR-12813-resistant SRD-16, -17, and -18 cells

CHO-7 or CHO-7/pInsig-2 cells were plated on day 0 at 1×10^6 cells/100 mm dish in medium A supplemented with 5% LPDS. On day 1, cells were refed the identical medium containing 0.3 mg/ml EMS. After incubation for 16 h at 37°C, cells were washed twice with PBS, trypsinized, and split 1:10 in medium A containing 5% LPDS. After 3 days (to allow expression of altered phenotypes), the cells were washed and refed medium A containing 5% LPDS and 10 μM SR-12813. Fresh medium was added to the cells every 2 days until colonies formed. On day 28, the surviving colonies were isolated with cloning cylinders and allowed to proliferate. The most vigorous SR-12813-resistant colonies were cloned by limiting dilution and designated SRD-16, -17, and -18.

Transient transfection of CHO-7 cells

Transfection of CHO-7 cells with FuGENE-6 transfection reagent (Roche) was performed as described (9). Conditions of the incubations are described in the figure legends. At the end of the incubations, triplicate dishes of cells for each variable were harvested and pooled for analysis.

Ubiquitination

Conditions of the incubations are described in the figure legends. At the end of the incubations, the cells were harvested and lysed in detergent-containing buffer, and immunoprecipitations were carried out with either polyclonal antibodies against the catalytic domain of human reductase or monoclonal anti-T7 IgG-coupled agarose beads (Novagen) against transfected reductase as described previously (8). Aliquots of the immunoprecipitates were subjected to SDS-PAGE on 8% gels, transferred to nitrocellulose membranes, and subjected to immunoblot analysis.

Cell fractionation and immunoblot analysis

Triplicate dishes of cells were used to isolate membrane fractions and nuclear extract fractions as described previously (16). Aliquots of nuclear extract and membrane fractions were subjected to 8% SDS-PAGE; the proteins were transferred to Hybond-C extra nitrocellulose filters (Millipore) and subjected to immunoblot analysis (16). Primary antibodies used for immunoblotting are as follows: IgG-7D4, a mouse monoclonal antibody against the NH_2 terminus of hamster SREBP-2 (31); IgG-A9, a mouse monoclonal antibody against the catalytic domain of hamster reductase (32); IgG-9E10, a mouse monoclonal antibody against c-Myc purified from the culture medium of hybridoma clone 9E10 (American Type Culture Collection); mouse monoclonal anti-T7-Tag IgG (Novagen); rabbit polyclonal anti-T7-Tag IgG (Bethyl Laboratories); monoclonal anti-hemagglutinin (HA) IgG (Sigma); and IgG-P4D1, a mouse monoclonal antibody against bovine ubiquitin (Santa Cruz Biotechnology).

PCR amplification and cloning of HMG-CoA reductase cDNA from SRD-16, -17, and -18 cells

Total RNA was isolated from CHO-7, CHO-7/pInsig-2, and SRD cells using the RNeasy kit (Qiagen) according to the manufacturer's instructions and subjected to reverse transcription reactions. First-strand cDNA was used to obtain PCR-amplified fragments containing nucleotides 4–823, 599–1,597, 871–2,418, and 2,353–2,661 of the reductase cDNA with the following forward and reverse primers, respectively: 5′-TTGTCACGACTTTTCCGTATG-3′ and 5′-CTATCCATCGACTGTGAGCAT-3′; 5′-CTGTGCTTGCCAACTACTTCGTGT-3′ and 5′-TATATCCGATCACATTCTCACAG-3′; 5′-TTGGGACTGGATGAAGATGTGT-3′ and 5′-ACCACCCACAGTTCCTATCTCTAT-3′; and 5′-TGCAGCAAACATCGTCA-3′ and 5′-CCATCAAAGGAGCCCGTAAAT-3′. PCR-amplified fragments (corresponding to nucleotides 124–327 and 817–1,120 of the reductase cDNA) were generated from genomic DNA isolated from the same cell lines using the following sets of forward and reverse primers: 5′-AAGATCTGTGGTTGGAATTACGAGTGC-3′ and 5′-GACTGTACTAAAGACAAAACTTGAG-3′; and 5′-TTGGGACTGGATGAAGATGTGT-3′ and 5′-GAGGCTCCCGTCTACAACAGT-3′. The resulting PCR products were subcloned into the pCRII vector (Invitrogen), and 10–30 individual clones were subjected to DNA sequencing to identify potential mutations in the reductase.

Plasmids

The following recombinant expression plasmids have been described as indicated: pCMV-HMG-Red-T7 and pCMV-HMG-Red-T7 (TM 1–8), which encode wild-type full-length or truncated (transmembrane helices 1–8) hamster reductase, respectively, followed by three copies of a T7 epitope tag under transcriptional control of the cytomegalovirus (CMV) promoter (8, 9); and pCMV-Insig-1-Myc, encoding human Insig-1, followed by six tandem copies of a c-Myc epitope tag under the control of the CMV promoter (21). The S60N, G87R, and A333P mutations were introduced into pCMV-HMG-Red-T7 and pCMV-HMG-Red-T7 (TM1–8) by site-directed mutagenesis using the QuikChange XL kit (Stratagene) and the following primer pairs: 5′-GAGGAGGATGTATTGAGCAATGACATCATCATCC-3′ and 5′-GGATGATGATGTCATTGCTCAATACATCCTCCTC-3′; 5′-CCAGAACTTACGTCAGCTTAGGTCGAAGTATATTTTAGG-3′ and 5′-CCTAAAATATACTTCGACCTAAGCTGACGTAAGTTCTGG-3′; and 5′-GCTTAGCTTTTCTGTTGCCTGTCAAGTACATTTTCTTTG-3′ and 5′-CAAAGAAAATGTACTTGACAGGCAACAGAAAAGCTAAGC-3′. The integrity of each plasmid was confirmed by DNA sequencing.

Blue native-PAGE

SRD-13A cells were set up for experiments and transfected as described in the legend to Fig. 5 below, after which they were harvested for preparation of a 1×10^5 *g* membrane pellet. The membrane pellet was then solubilized in buffer containing 1% (w/v) digitonin and subjected to centrifugation at 20,000 *g*. One aliquot of the resulting supernatant was mixed with a 6-amino-*n*-hexanoic acid-containing buffer and subjected to electrophoresis on a 4–16% blue native gel as described (21). A second aliquot of the supernatant was mixed with SDS-containing buffer and subjected to 8% SDS-PAGE.

RESULTS

CHO-7 [a subline of CHO-K1 cells selected for growth in LPDS-containing medium (33)] and CHO-7/pInsig-2 (CHO-7 cells expressing multiple copies of an Insig-2 cDNA) cells were mutagenized with EMS and subjected to selection for 4 weeks in medium containing LPDS and 10 μM SR-12813. Three SR-12813-resistant clones were isolated, expanded, and designated SRD-16, -17, and -18 (for sterol regulatory defective). SRD-16 cells were derived from CHO-7/pInsig-2 cells, whereas SRD-17 and -18 cells resulted from mutagenesis and selection of CHO-7 cells. **Figure 1A** shows that growth of parental CHO-7 and CHO-7/pInsig-2 cells, but not that of the mutant cells, was prevented when LPDS-containing culture medium was supplemented with 10 μM SR-12813. The addition of cholesterol restored the growth of parental cells in SR-12813, indicating that cell death was caused by cholesterol depletion.

In the experiment shown in Fig. 1B, wild-type and mutant cells were incubated for 16 h in medium containing LPDS, the reductase inhibitor compactin, and a low level of mevalonate, the product of reductase. The low level of mevalonate permits the synthesis of nonsterol mevalonate-derived products, such as the prenyl groups that are found attached to many cellular proteins, but is not sufficient to produce normal amounts of cholesterol (5). The resultant sterol-depleted cells were then subjected to 5 h treatments with SR-12813 or 25-HC, after which they were harvested and separated into membrane and nuclear extract fractions. Aliquots of each fraction were subjected to SDS-PAGE and immunoblotted with antibodies against reductase and SREBP-2, the SREBP family member that is most dedicated to cholesterol synthesis (34). Treatment of CHO-7/pInsig-2 and CHO-7 cells with either 25-HC or SR-12813 decreased the amount of reductase in membranes (Fig. 1B, top panel, lanes 1–3, 7–9), indicative of accelerated degradation of the enzyme. In contrast, neither 25-HC nor SR-12813 stimulated degradation of the reductase in SRD-16, -17, or -18 cells (Fig. 1B, top panel, lanes 4–6, 10–15). Treatment with 25-HC caused the disappearance of nuclear SREBP-2 in parental and mutant cells (Fig. 1B, bottom panel, lanes 2, 5, 8, 11, 14). On the other hand, SR-12813 failed to block SREBP-2 processing in any of the cell lines (Fig. 1B, bottom panel, lanes 3, 6, 9, 12, 15).

The experiment shown in Fig. 1C was designed to determine the ubiquitination state of reductase in wild-type and mutant cells treated with 25-HC. Sterol-depleted cells

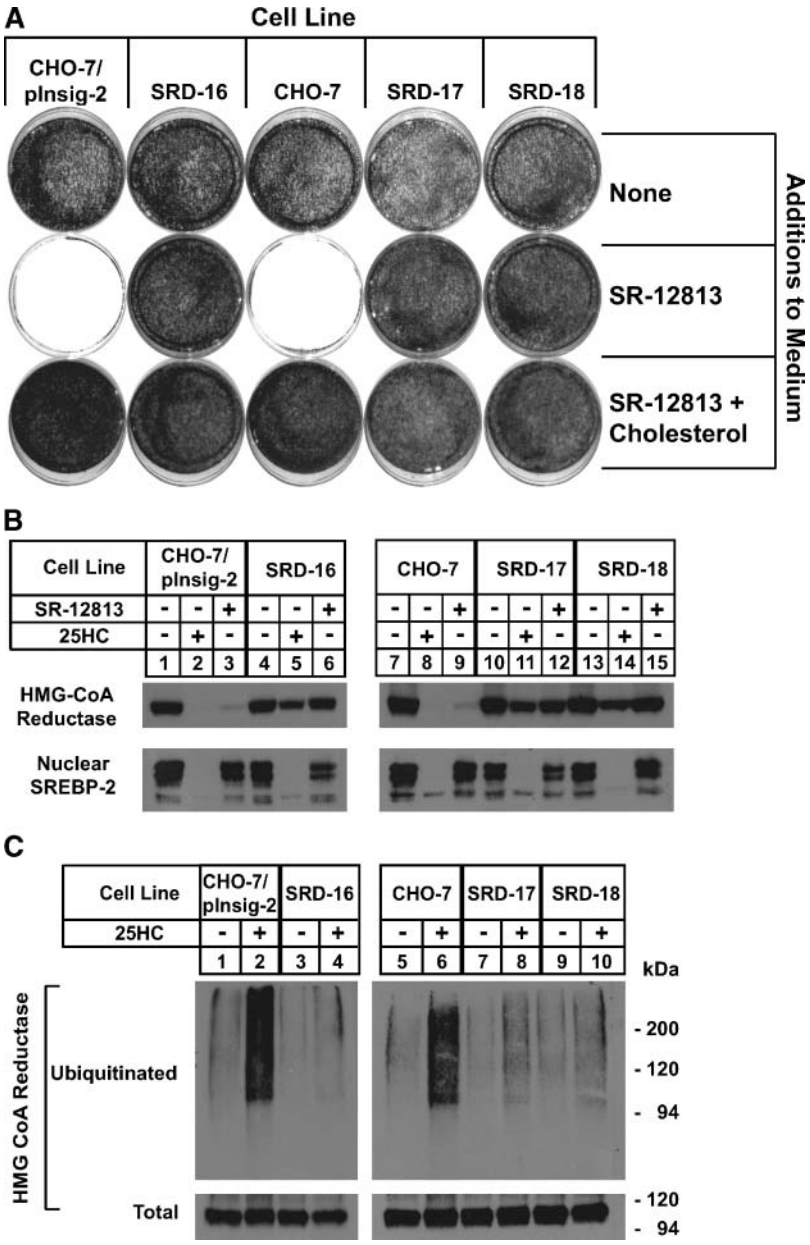

Fig. 1. Characterization of mutant Chinese hamster ovary (CHO) cells resistant to SR-12813. A: CHO-7, CHO-7/pInsig-2, and SRD-16, -17, and -18 cells were set up on day 0 at 4×10^4 cells per 60 mm dish in medium A supplemented with 5% lipoprotein-deficient serum (LPDS). On day 1, cells were washed with PBS and refed medium A containing 5% LPDS in the absence or presence of 10 μM SR-12813. Some of the SR-12813-treated cells also received 25 μM cholesterol. Cells were refed fresh medium every 2 days. On day 10, cells were washed, fixed in 95% ethanol, and stained with crystal violet. B: CHO-7 cells were set up on day 0 at 5×10^5 cells per 100 mm dish in medium A containing 5% LPDS. On day 2, cells were refed medium A supplemented with 5% LPDS, 10 μM sodium compactin, and 50 μM sodium mevalonate. After 16 h at 37°C, cells were switched to medium A containing 5% LPDS and 10 μM compactin in the absence or presence of either 25-hydroxycholesterol (25-HC) or SR-12813 plus 10 mM mevalonate as indicated. After 5 h at 37°C, the cells were harvested and subjected to subcellular fractionation. Aliquots of the membrane (13 μg of protein/lane) and nuclear extract (15 μg of protein/lane) fractions were subjected to SDS-PAGE and transferred to nitrocellulose membranes, and immunoblot analysis was carried out with 5 μg/ml monoclonal IgG-A9 (against reductase) or 5 μg/ml monoclonal IgG-7D4 [against sterol-regulatory element binding protein-2 (SREBP-2)]. C: CHO-7 cells were set up for experiments and depleted of sterols as described for A. Sterol-depleted cells were subsequently switched to medium A containing 5% LPDS, 10 μM compactin, and 10 μM MG-132 in the absence or presence of 2.5 μM 25-HC plus 10 mM mevalonate as indicated. After 2 h, the cells were harvested, lysed, and subjected to immunoprecipitation with anti-reductase polyclonal antibodies. Immunoblot analysis was carried out with 5 μg/ml IgG-A9 or 0.2 μg/ml monoclonal IgG-P4D1 (against ubiquitin).

were subjected to 25-HC treatment in the presence of MG-132, a proteasome inhibitor that blocks the degradation of ubiquitinated proteins. After treatments, cells were harvested, and detergent lysates were prepared and subsequently immunoprecipitated with polyclonal antibodies against reductase. Immunoblotting with anti-ubiquitin revealed the accumulation of high molecular weight material in reductase immunoprecipitates from CHO-7/pInsig-2 and CHO-7 cells subjected to 25-HC treatment (Fig. 1C, top panel, lanes 2, 6), indicating that reductase had become ubiquitinated. This 25-HC-dependent ubiquitination of reductase was markedly diminished in SRD cells (Fig. 1C, top panel, lanes 4, 8, 10), a result consistent with their inability to degrade reductase in the presence of the sterol (Fig. 1B).

Considering that reductase degradation, but not SREBP-2 processing, is resistant to 25-HC-mediated regulation in SRD cells and the propensity of EMS mutagenesis to generate point mutations, we hypothesized that this resistance was a consequence of mutation(s) in reductase. Thus, total RNA was isolated from SRD cells and used to synthesize first-strand cDNA, from which the cDNA encoding reductase was amplified by PCR. The resulting products were subcloned, and 10–30 individual clones were subjected to DNA sequencing, which revealed a G-to-A or G-to-C substitution in reductase mRNAs from each cell line. These substitutions resulted in changes of Ser-60 (AGT) to Asp (AAT), Gly-87 (GGG) to Arg (AGG), and Ala-333 (GCT) to Pro (CCT) for SRD-16, -17, and -18 cells, respectively. The frequency of these changes in the randomly sequenced cDNA clones was close to 50% (8 of 16 for SRD-16, 8 of 12 for SRD-17, and 13 of 30 for SRD-18). This strongly indicates that each of the SRD cell lines is heterozygous for its respective mutation. This 50% frequency was confirmed by sequencing multiple clones of PCR-amplified fragments from genomic DNA

that included each codon (5 of 14 for SRD-16, 6 of 10 for SRD-17, and 5 of 10 for SRD-18). As shown in **Fig. 2A**, Ser-60 and Ala-333 localize to transmembrane helices 2 and 8 of reductase, respectively; Gly-87 lies within the cytosolic loop that separates helices 2 and 3. The amino acid sequence alignment in Fig. 2B shows that Ser-60, Gly-87, and Ala-333 are conserved between hamster, human, *Xenopus*, zebrafish-1, and sea urchin reductase. Notably, Ser-60 is not conserved in zebrafish-2 reductase, one of two reductase isozymes expressed in zebrafish (35). Gly-87 is also present in the *Drosophila* reductase. Even though Ser-60 and Gly-87 localize to the sterol-sensing domain of reductase, neither amino acid is present in the corresponding region of SCAP's sterol-sensing domain.

Experiments were next designed to directly demonstrate that the S60N, G87R, and A333P mutations impart resistance of reductase to sterol-stimulated ubiquitination (**Fig. 3**) and degradation (**Fig. 4A, B**). CHO-7 cells were transfected with wild-type or mutant versions (G87R, A333P, or S60N) of pCMV-HMG-Red-T7, an expression plasmid that encodes full-length reductase followed by three copies of a T7 epitope tag (8). The sensitivity of ubiquitin detection was enhanced by the additional transfection of pEFla-HA-ubiquitin, which encodes human ubiquitin with an NH_2-terminal tag consisting of two copies of the HA epitope. After sterol depletion, the cells were subjected to treatments with MG-132 and various concentrations of 25-HC. Transfected reductase was immunoprecipitated from detergent lysates using anti-T7-coupled agarose beads, and the resulting precipitates were immunoblotted with antibodies against T7 and HA for reductase and ubiquitin, respectively. When transfected alone, wild-type, S60N, G87R, and A333P reductase failed to become ubiquitinated in the presence of 2.5 μM 25-HC (Fig. 3A–C, top panels, lanes a, b, g, h). Dose-dependent, 25-HC-induced ubiquitination of wild-type reductase was restored upon coexpression of pCMV-Insig-1-Myc, which encodes human Insig-1 followed by six copies of the c-Myc epitope (Fig. 3A–C, top panels,

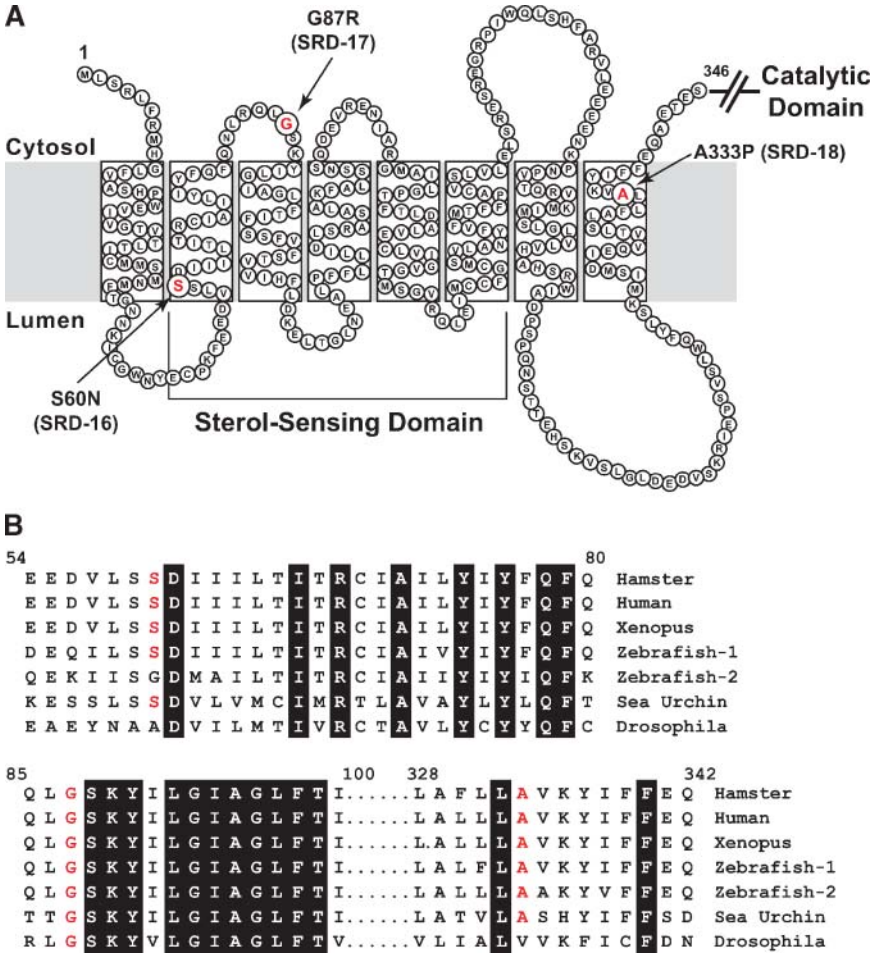

Fig. 2. Localization and conservation of amino acid residues in HMG-CoA reductase membrane domain. A: Amino acid sequence and topology of the membrane domain of hamster HMG-CoA reductase. The amino acid residues that are mutated in SRD-16, -17, and -18 cells are enlarged, shown in red, and denoted by arrows. B: Comparison of amino acid residues in hamster, human, *Xenopus*, zebrafish-1, zebrafish-2, sea urchin, and *Drosophila* HMG-CoA reductase surrounding Ser-60, Gly-87, and Ala-333 (shown in red). GenBank accession numbers are P00347, NP000850, P20715, XP684400, AI497311, NP999724, and P14773, respectively. Residues that are identical in all six proteins are highlighted in black.

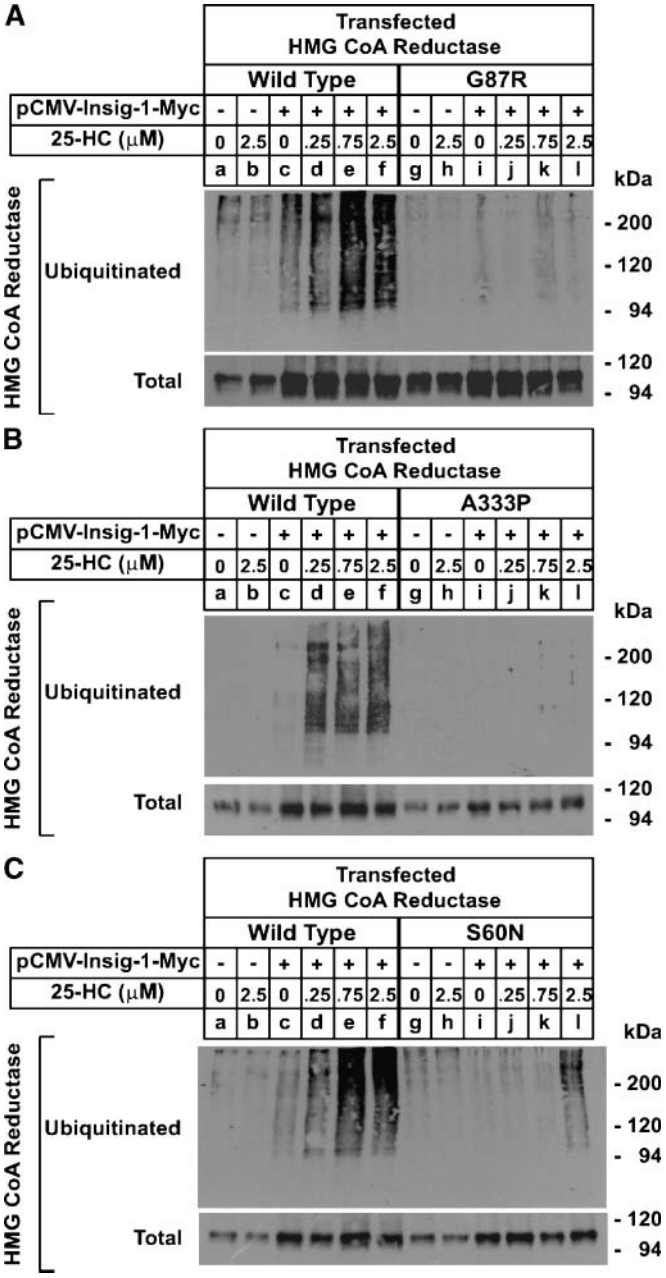

Fig. 3. Ubiquitination of the S60N, G87R, and A333P versions of HMG-CoA reductase. CHO-7 cells were set up on day 0 at 5×10^5 cells per 60 mm dish in medium A containing 5% LPDS. On day 1, the cells were transfected with 1 μg of wild type (panels A–C; lanes a–f), G87R (panel A; lanes g–l), A333P (panel B; lanes g–l), or S60N (panel C; lanes g–l) pCMV-HMG-Red-T7 together with 0.1 μg of pEF1a-HA-ubiquitin in 2 ml of medium A containing 5% LPDS. The total DNA in each dish was adjusted to 3 μg by the addition of pcDNA3 mock vector. Six hours after transfection, the cells were depleted of sterols by the direct addition of 2 ml of medium A containing 5% LPDS, 10 μM compactin, and 50 μM mevalonate (final concentrations). After 16 h at 37°C, cells were switched to medium A containing 5% LPDS, 10 μM compactin, 10 μM MG-132, and the indicated concentration of 25-HC. After incubation for 2 h at 37°C, the cells were harvested, lysed, and subjected sequentially to immunoprecipitation with anti-T7-coupled agarose beads and SDS-PAGE. Immunoblot analysis was carried out with a 1:500 dilution of monoclonal IgG-hemagglutinin (against ubiquitin) or 1 μg/ml monoclonal anti-T7 IgG (against reductase).

lanes d–f). Regulated ubiquitination was nearly absent for the G87R and A333P versions of reductase, and S60N reductase only became ubiquitinated with the highest level (2.5 μM) of 25-HC (Fig. 3A–C, top panels, lanes j–l).

Similar results were obtained for reductase degradation (Fig. 4A, B). In these experiments, sterol-depleted CHO-7 cells transfected with wild-type or mutant reductase were incubated with various amounts of 25-HC (Fig. 4A) or lanosterol (Fig. 4B), a cholesterol synthesis intermediate that stimulates the degradation of endogenous reductase (36). When transfected alone, degradation of wild-type, S60N, G87R, or A333P reductase was not accelerated by 25-HC (Fig. 4A, top panels, lanes a, b, g, h) or lanosterol (Fig. 4B, top panels, lanes m, n, s, t). Coexpression of pCMV-Insig-1-Myc restored the degradation of wild-type reductase in the presence of 25-HC (Fig. 4A, top panels, lanes d–f) or lanosterol (Fig. 4B, top panels, lanes p–r), but G87R, A333P, and S60N reductase remained largely resistant to degradation (Fig. 4A, B, top panels, lanes j–l, v–x).

Figure 4C shows a growth experiment designed to determine whether the S60N, G87R, and A333P mutations in reductase confer an SR-12813-resistant phenotype. CHO-7 cells were transfected with wild-type or mutant versions of pCMV-HMG-Red-T7. The plasmids also encode *neo*, a gene that confers resistance to G418. After transfection and selection of transformants with G418, the cells were grown for an additional 2 weeks in medium containing LPDS in the absence or presence of SR-12813. Transfection of the control plasmid or wild-type reductase did not permit the cells to grow in medium containing SR-12813, whereas transfection of the mutant forms of reductase allowed cell growth in the presence of the drug.

In previous studies, blue native-PAGE was used to visualize sterol-dependent complexes between Insig-1 and the membrane domain of reductase, which is necessary and sufficient for regulated degradation (3, 27, 37). Considering the results of Figs. 3 and 4, which show that Ser-60, Gly-87, and Ala-333 in reductase are essential for Insig-mediated ubiquitination and degradation, we used blue native-PAGE to determine whether the most robust mutation (G87R) decreases the binding between the membrane domain of reductase and Insig-1. In **Fig. 5**, SCAP-deficient SRD-13A cells were transfected with various combinations of pCMV-Insig-1-Myc and wild-type or mutant versions of pCMV-HMG-Red-T7 (TM 1–8), which encodes a truncated reductase that contains the entire membrane domain (Fig. 2A) but lacks the catalytic domain. After sterol depletion with hydroxypropyl-β-cyclodextrin and pretreatment with MG-132, the cells were subjected to an additional incubation in the absence or presence of 25-HC. The cells were subsequently harvested, and membrane fractions were isolated and solubilized with digitonin. Soluble material was mixed with Coomassie Blue and 6-amino-*n*-hexanoic acid (to impart a negative charge and prevent the precipitation of proteins), subjected to PAGE, and immunoblotted with antibodies against the T7 and Myc epitopes. The anti-T7 immunoblot of the native gel revealed that when transfected alone, the membrane domain of reductase appeared as a single band

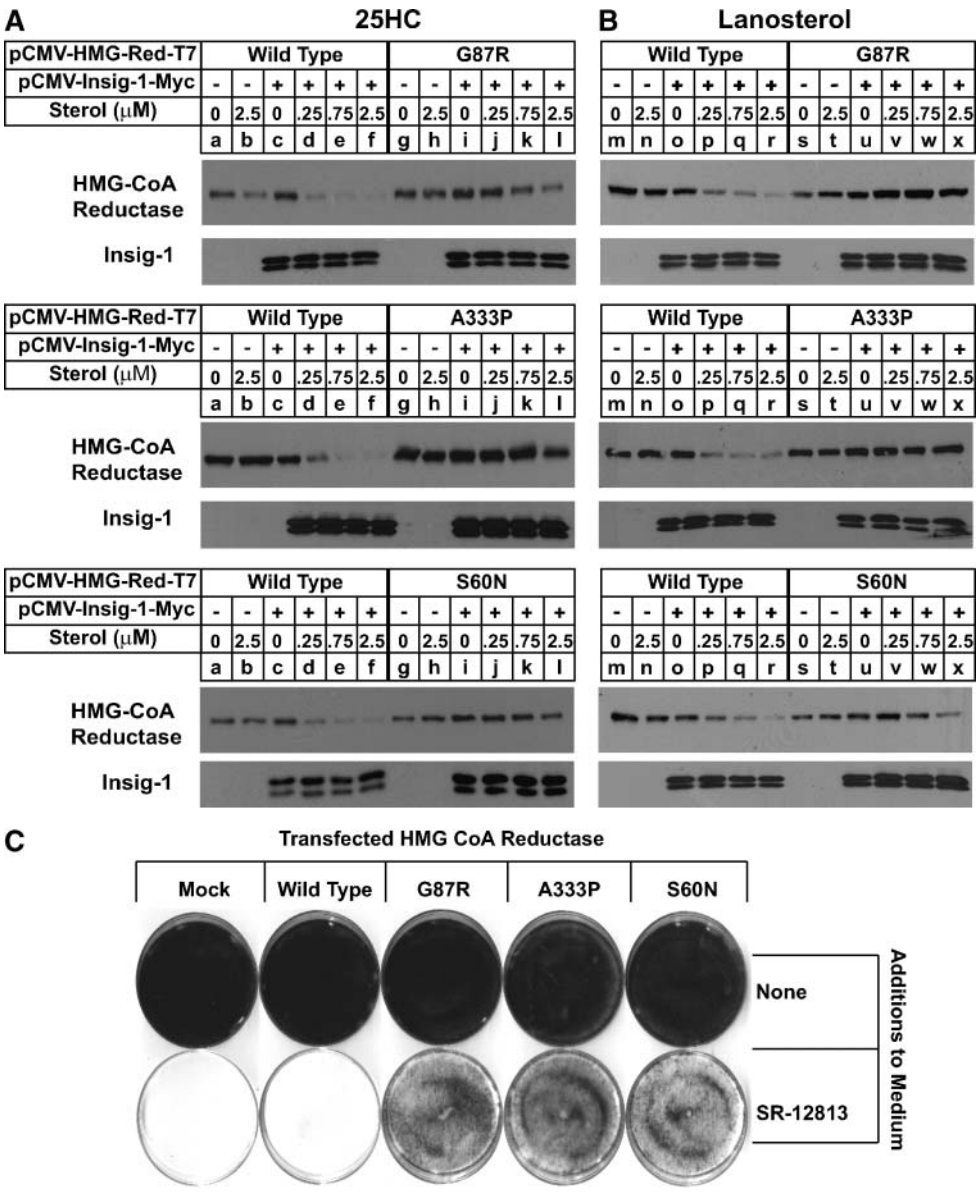

Fig. 4. Properties of S60N, G87R, and A333P HMG-CoA reductase in transfected cells. A, B: CHO-7 cells were set up and transfected as described for Fig. 3 with 1 μg of wild-type, S60N, G87R, or A333P pCMV-HMG-Red-T7 in the absence or presence of 30 ng of pCMV-Insig-1-Myc. After sterol depletion for 16 h at 37°C, cells were switched to medium A containing 5% LPDS, 10 μM compactin, and the indicated concentration of 25-HC (A) or lanosterol (B) plus 10 mM mevalonate. After incubation for 5 h at 37°C, cells were harvested, membrane fractions were prepared, and aliquots (3–6 μg) were subjected to SDS-PAGE. Immunoblot analysis was carried out with 1 μg/ml monoclonal anti-T7 IgG (against reductase) and 3 μg/ml monoclonal IgG-9E10 (against Insig-1) antibodies. C: CHO-7 cells were set up on day 0 at 5×10^5 cells per 60 mm dish in medium A containing 5% LPDS. On day 1, the cells were transfected with 1 μg of either pcDNA3 (Mock) or wild-type, S60N, G87R, or A333P pCMV-HMG-Red-T7. All of the plasmids contained the G418 resistance gene *neo*. On day 2, the cells were switched to medium A containing 5% LPDS and 0.7 mg/ml G418 and refed every 2 days. No cells survived in control dishes that did not receive any plasmid during transfection. On day 12, the surviving cells were trypsinized and pooled, and triplicate sets of dishes were set up in medium A containing 5% LPDS. On day 13, cells were switched to identical medium in the absence or presence of 10 μM SR-12813. On day 22, cells were fixed and stained as described for Fig. 1.

in the absence or presence of 25-HC (Fig. 5, top panel, lanes 3, 4). This band was designated unbound reductase. When Insig-1 was coexpressed, some of the reductase migrated more slowly (Fig. 5, top panel, lane 5), and this band was designated the reductase-Insig-1 complex. With 25-HC treatment, unbound reductase almost completely disappeared and the amount of reductase in complex with Insig-1 increased (Fig. 5, top panel, lanes 6 and 7). In contrast, migration of the G87R version of the reductase membrane domain was not retarded in the presence of

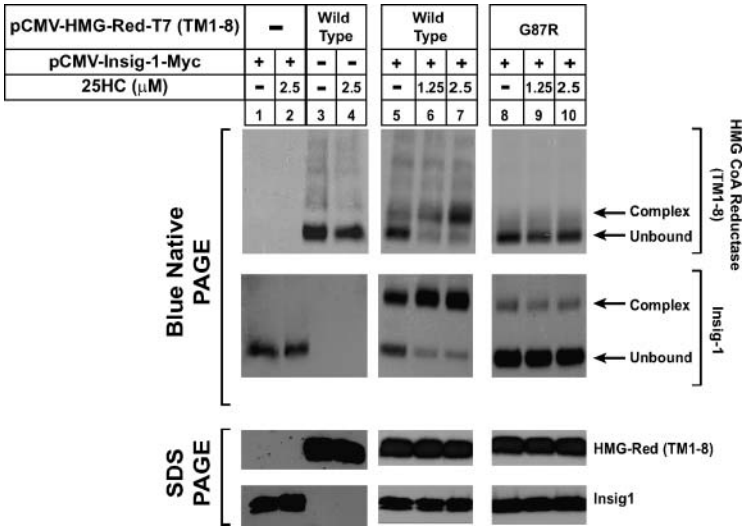

Fig. 5. Introduction of the G87R mutation into the membrane domain of HMG-CoA reductase impairs binding to Insig-1 in the presence of 25-HC. SRD-13A cells were set up for experiments on day 0 at 7×10^5 cells per 100 mm dish. On day 2, the cells were transfected in medium A containing 5% fetal calf serum as described for Fig. 3 with 60 ng of pCMV-Insig-1-Myc in the absence or presence of 4 μg of wild-type or G87R pCMV-HMG-Red-T7(TM1–8) as indicated. After incubation for 16 h at 37°C, cells were switched to medium A containing 5% LPDS, 1% hydroxypropyl-β-cyclodextrin, and 10 μM compactin and incubated for 1 h at 37°C. The cells were then washed, switched to identical medium (without hydroxypropyl-β-cyclodextrin) supplemented with 10 μM MG-132, and incubated for 1 h at 37°C. This was followed by incubation for an additional 1 h in the same medium with or without 1 μg/ml 25-HC plus 10 mM mevalonate as indicated. The cells were subsequently harvested and subjected to subcellular fractionation. Aliquots of the 1×10^5 *g* membrane pellet were solubilized in 1% digitonin and subjected to blue native-PAGE (middle panels) or SDS-PAGE (bottom panels). Immunoblot analysis was carried out with 1 μg/ml polyclonal anti-T7 IgG (against reductase) and 5 μg/ml monoclonal IgG-9E10 (against Insig-1).

Insig-1 and sterols (Fig. 5, top panel, lanes 8–10). A similar result was observed in the anti-Myc blots of the native gel (Fig. 5, middle panel). 25-HC caused a complete disappearance of unbound Insig-1 upon coexpression of the wild type but not the G87R mutant of the reductase membrane domain (Fig. 5, middle panel, lanes 8–10). Immunoblots of SDS-PAGE gels revealed constant expression of Insig-1, wild-type reductase, and mutant G87R reductase, regardless of the absence or presence of 25-HC (Fig. 5, bottom panel). Together, these results indicate that the G87R mutation disrupts the binding of reductase to Insigs, thereby rendering the enzyme resistant to sterol-regulated ubiquitination and degradation.

DISCUSSION

The current data document the isolation of three independently derived lines of mutant CHO cells resistant to SR-12813, which inhibits cholesterol synthesis by stimulating Insig-dependent ubiquitination and degradation of HMG-CoA reductase. Neither SR-12813 nor the oxysterol 25-HC stimulated the degradation and ubiquitination of endogenous reductase in the mutant cells (Fig. 1B, C), which are designated SRD-16, -17, and -18. DNA sequencing revealed that SRD-16, -17, and -18 cells exhibit a G-to-A or G-to-C substitution in codons 60, 87, and 333 of reductase, respectively, that result in changes of Ser-60 to Asn, Gly-87 to Arg, and Ala-333 to Pro. Transient transfection assays revealed that the S60N, G87R, and A333P mutations render reductase refractory to Insig-mediated, sterol-accelerated ubiquitination (Fig. 3) and degradation (Fig. 4A, B). Moreover, overexpression of a cDNA encoding full-length S60N, G87R, or A333P reductase allowed the growth of wild-type cells in SR-12813-supplemented medium (Fig. 4C). Considered together, these results identify Ser-60, Gly-87, and Ala-333 as key residues for the regulated ubiquitination and degradation of reductase and demonstrate that their mutation confers a dominant, SR-12813-resistant phenotype.

The determining factor for the degradation of reductase is sterol-induced binding of the enzyme to Insigs, which are carriers of the membrane-anchored gp78 ubiquitin ligase that facilitates reductase ubiquitination (10). Interactions between reductase and Insigs are mediated entirely by the membrane domain of reductase (9), which may explain the high degree of conservation observed in the region across species (Fig. 2B). Indeed, sterol-regulated formation of the reductase-Insig complex is blocked by mutation of a YIYF tetrapeptide sequence that is located in the second membrane-spanning region of reductase (8). Similarly, Ser-60, Gly-87, and Ala-333 localize to the membrane domain of reductase (Fig. 2A), and introducing the G87 mutation into the membrane domain of reductase impaired sterol-regulated complex formation with Insig-1 (Fig. 5). It should be noted that

native gels revealed that the A333P and S60N mutations in the membrane domain of reductase similarly disrupted reductase-Insig binding; however, this effect was not as pronounced as that observed with the G87R mutant.

In unpublished studies, we found that the resistance of S60N and G87R reductase is attributable to loss of the Ser at residue 60 and the Gly at residue 87, respectively. This is indicated by substitution experiments, which showed that replacing Gly-87 with lysine or Ala and replacing Ser-60 with threonine or glutamine produced a sterol-resistant phenotype. In contrast, the phenotype of A333P reductase likely results from the acquisition of a Pro, because replacement of Ala-333 with Gly did not produce sterol resistance (unpublished observations). Native gels indicate the Pro residue imparts a significant structural change in the membrane domain of reductase that impedes Insig binding (unpublished observations). However, this structural alteration does not appear to abrogate any catalytic activity of reductase, which is indicated by the observation that expression of A333P reductase in wild-type cells allows growth in SR-12813-containing medium (Fig. 4C). Further insight into the effects of A333P and other mutations on the membrane domain of reductase will require detailed structural studies by X-ray crystallography or NMR.

The selection for SR-12813 resistance used in the current study is unbiased. This selection produced three resistant cell lines with point mutations in the membrane domain of reductase, and all three mutations conferred resistance to sterol-stimulated, Insig-dependent ubiquitination. These findings provide strong and unbiased support for the conclusion that reductase degradation absolutely requires reductase-Insig interaction through the membrane domains of the two proteins. The predominance of reductase mutations found in this study, and the isolation of Insig mutants in previous mutagenesis experiments [i.e., SRD-14 and SRD-15 (27, 38)], strongly suggest that the number of other proteins required specifically for reductase degradation is limited and that our understanding of this process is relatively complete.

The authors thank Drs. Michael S. Brown and Joseph L. Goldstein for critical evaluation of the manuscript and their continued encouragement and advice. The authors also thank Tammy Dinh and Kristi Garland for excellent technical assistance and Lisa Beatty for help with tissue culture. This work was supported by grants from the National Institutes of Health (Grant HL-20948) and the Perot Family Foundation. A.D.N. is supported by a Division of Cell and Molecular Biology Training Program grant (T32GM008203). R.A.D-B. is the recipient of a National Institutes of Health Mentored Minority Faculty Development Award (HL-70441), an Established Investigator Award from the American Heart Association (0540128N), and a Distinguished Young Investigator in Medical Research Award from the W. M. Keck Foundation.

REFERENCES

1. Goldstein, J. L., and M. S. Brown. 1990. Regulation of the mevalonate pathway. *Nature.* **343:** 425–430.
2. Roitelman, J., E. H. Olender, S. Bar-Nun, W. A. Dunn, Jr., and R. D. Simoni. 1992. Immunological evidence for eight spans in the membrane domain of 3-hydroxy-3-methylglutaryl coenzyme A reductase: implications for enzyme degradation in the endoplasmic reticulum. *J. Cell Biol.* **117:** 959–973.
3. Gil, G., J. R. Faust, D. J. Chin, J. L. Goldstein, and M. S. Brown. 1985. Membrane-bound domain of HMG CoA reductase is required for sterol-enhanced degradation of the enzyme. *Cell.* **41:** 249–258.
4. Liscum, L., J. Finer-Moore, R. M. Stroud, K. L. Luskey, M. S. Brown, and J. L. Goldstein. 1985. Domain structure of 3-hydroxy-3-methylglutaryl coenzyme A reductase, a glycoprotein of the endoplasmic reticulum. *J. Biol. Chem.* **260:** 522–530.
5. Brown, M. S., and J. L. Goldstein. 1980. Multivalent feedback regulation of HMG CoA reductase, a control mechanism coordinating isoprenoid synthesis and cell growth. *J. Lipid Res.* **21:** 505–517.
6. Nakanishi, M., J. L. Goldstein, and M. S. Brown. 1988. Multivalent control of 3-hydroxy-3-methylglutaryl coenzyme A reductase. Mevalonate-derived product inhibits translation of mRNA and accelerates degradation of enzyme. *J. Biol. Chem.* **263:** 8929–8937.
7. Roitelman, J., and R. D. Simoni. 1992. Distinct sterol and nonsterol signals for the regulated degradation of 3-hydroxy-3-methylglutaryl-CoA reductase. *J. Biol. Chem.* **267:** 25264–25273.
8. Sever, N., B. L. Song, D. Yabe, J. L. Goldstein, M. S. Brown, and R. A. DeBose-Boyd. 2003. Insig-dependent ubiquitination and degradation of mammalian 3-hydroxy-3-methylglutaryl-CoA reductase stimulated by sterols and geranylgeraniol. *J. Biol. Chem.* **278:** 52479–52490.
9. Sever, N., T. Yang, M. S. Brown, J. L. Goldstein, and R. A. DeBose-Boyd. 2003. Accelerated degradation of HMG CoA reductase mediated by binding of Insig-1 to its sterol-sensing domain. *Mol. Cell.* **11:** 25–33.
10. Song, B. L., N. Sever, and R. A. DeBose-Boyd. 2005. Gp78, a membrane-anchored ubiquitin ligase, associates with Insig-1 and couples sterol-regulated ubiquitination to degradation of HMG CoA reductase. *Mol. Cell.* **19:** 829–840.
11. Ravid, T., R. Doolman, R. Avner, D. Harats, and J. Roitelman. 2000. The ubiquitin-proteasome pathway mediates the regulated degradation of mammalian 3-hydroxy-3-methylglutaryl-coenzyme A reductase. *J. Biol. Chem.* **275:** 35840–35847.
12. Goldstein, J. L., R. A. DeBose-Boyd, and M. S. Brown. 2006. Protein sensors for membrane sterols. *Cell.* **124:** 35–46.
13. Nohturfft, A., M. S. Brown, and J. L. Goldstein. 1998. Topology of SREBP cleavage-activating protein, a polytopic membrane protein with a sterol-sensing domain. *J. Biol. Chem.* **273:** 17243–17250.
14. Sakai, J., A. Nohturfft, D. Cheng, Y. K. Ho, M. S. Brown, and J. L. Goldstein. 1997. Identification of complexes between the COOH-terminal domains of sterol regulatory element-binding proteins (SREBPs) and SREBP cleavage-activating protein. *J. Biol. Chem.* **272:** 20213–20221.
15. Brown, M. S., and J. L. Goldstein. 1997. The SREBP pathway: regulation of cholesterol metabolism by proteolysis of a membrane-bound transcription factor. *Cell.* **89:** 331–340.
16. DeBose-Boyd, R. A., M. S. Brown, W. P. Li, A. Nohturfft, J. L. Goldstein, and P. J. Espenshade. 1999. Transport-dependent proteolysis of SREBP: relocation of site-1 protease from Golgi to ER obviates the need for SREBP transport to Golgi. *Cell.* **99:** 703–712.
17. Nohturfft, A., D. Yabe, J. L. Goldstein, M. S. Brown, and P. J. Espenshade. 2000. Regulated step in cholesterol feedback localized to budding of SCAP from ER membranes. *Cell.* **102:** 315–323.
18. Sakai, J., E. A. Duncan, R. B. Rawson, X. Hua, M. S. Brown, and J. L. Goldstein. 1996. Sterol-regulated release of SREBP-2 from cell membranes requires two sequential cleavages, one within a transmembrane segment. *Cell.* **85:** 1037–1046.
19. Adams, C. M., J. Reitz, J. K. De Brabander, J. D. Feramisco, L. Li, M. S. Brown, and J. L. Goldstein. 2004. Cholesterol and 25-hydroxycholesterol inhibit activation of SREBPs by different mechanisms, both involving SCAP and Insigs. *J. Biol. Chem.* **279:** 52772–52780.
20. Yabe, D., M. S. Brown, and J. L. Goldstein. 2002. Insig-2, a second endoplasmic reticulum protein that binds SCAP and blocks export of sterol regulatory element-binding proteins. *Proc. Natl. Acad. Sci. USA.* **99:** 12753–12758.
21. Yang, T., P. J. Espenshade, M. E. Wright, D. Yabe, Y. Gong, R. Aebersold, J. L. Goldstein, and M. S. Brown. 2002. Crucial step in cholesterol homeostasis: sterols promote binding of SCAP to INSIG-1, a membrane protein that facilitates retention of SREBPs in ER. *Cell.* **110:** 489–500.

22. Hua, X., A. Nohturfft, J. L. Goldstein, and M. S. Brown. 1996. Sterol resistance in CHO cells traced to point mutation in SREBP cleavage-activating protein. *Cell.* **87:** 415–426.
23. Brown, M. S., and J. L. Goldstein. 1999. A proteolytic pathway that controls the cholesterol content of membranes, cells, and blood. *Proc. Natl. Acad. Sci. USA.* **96:** 11041–11048.
24. Kuwabara, P. E., and M. Labouesse. 2002. The sterol-sensing domain: multiple families, a unique role? *Trends Genet.* **18:** 193–201.
25. Nohturfft, A., M. S. Brown, and J. L. Goldstein. 1998. Sterols regulate processing of carbohydrate chains of wild-type SREBP cleavage-activating protein (SCAP), but not sterol-resistant mutants Y298C or D443N. *Proc. Natl. Acad. Sci. USA.* **95:** 12848–12853.
26. Nohturfft, A., X. Hua, M. S. Brown, and J. L. Goldstein. 1996. Recurrent G-to-A substitution in a single codon of SREBP cleavage-activating protein causes sterol resistance in three mutant Chinese hamster ovary cell lines. *Proc. Natl. Acad. Sci. USA.* **93:** 13709–13714.
27. Sever, N., P. C. W. Lee, B. L. Song, R. B. Rawson, and R. A. DeBose-Boyd. 2004. Isolation of mutant cells lacking Insig-1 through selection with SR-12813, an agent that stimulates degradation of 3-hydroxy-3-methylglutaryl-coenzyme A reductase. *J. Biol. Chem.* **279:** 43136–43147.
28. Goldstein, J. L., S. K. Basu, and M. S. Brown. 1983. Receptor-mediated endocytosis of low-density lipoprotein in cultured cells. *Methods Enzymol.* **98:** 241–260.
29. Yabe, D., Z. P. Xia, C. M. Adams, and R. B. Rawson. 2002. Three mutations in sterol-sensing domain of SCAP block interaction with Insig and render SREBP cleavage insensitive to sterols. *Proc. Natl. Acad. Sci. USA.* **99:** 16672–16677.
30. Rawson, R. B., R. DeBose-Boyd, J. L. Goldstein, and M. S. Brown. 1999. Failure to cleave sterol regulatory element-binding proteins (SREBPs) causes cholesterol auxotrophy in Chinese hamster ovary cells with genetic absence of SREBP cleavage-activating protein. *J. Biol. Chem.* **274:** 28549–28556.
31. Yang, J., M. S. Brown, Y. K. Ho, and J. L. Goldstein. 1995. Three different rearrangements in a single intron truncate sterol regulatory element binding protein-2 and produce sterol-resistant phenotype in three cell lines. Role of introns in protein evolution. *J. Biol. Chem.* **270:** 12152–12161.
32. Liscum, L., K. L. Luskey, D. J. Chin, Y. K. Ho, J. L. Goldstein, and M. S. Brown. 1983. Regulation of 3-hydroxy-3-methylglutaryl coenzyme A reductase and its mRNA in rat liver as studied with a monoclonal antibody and a cDNA probe. *J. Biol. Chem.* **258:** 8450–8455.
33. Metherall, J. E., J. L. Goldstein, K. L. Luskey, and M. S. Brown. 1989. Loss of transcriptional repression of three sterol-regulated genes in mutant hamster cells. *J. Biol. Chem.* **264:** 15634–15641.
34. Horton, J. D., J. L. Goldstein, and M. S. Brown. 2002. SREBPs: activators of the complete program of cholesterol and fatty acid synthesis in the liver. *J. Clin. Invest.* **109:** 1125–1131.
35. Thorpe, J. L., M. Doitsidou, S. Y. Ho, E. Raz, and S. A. Farber. 2004. Germ cell migration in zebrafish is dependent on HMGCoA reductase activity and prenylation. *Dev. Cell.* **6:** 295–302.
36. Song, B. L., N. B. Javitt, and R. A. DeBose-Boyd. 2005. Insig-mediated degradation of HMG CoA reductase stimulated by lanosterol, an intermediate in the synthesis of cholesterol. *Cell Metab.* **1:** 179–189.
37. Skalnik, D. G., H. Narita, C. Kent, and R. D. Simoni. 1988. The membrane domain of 3-hydroxy-3-methylglutaryl-coenzyme A reductase confers endoplasmic reticulum localization and sterol-regulated degradation onto beta-galactosidase. *J. Biol. Chem.* **263:** 6836–6841.
38. Lee, P. C. W., N. Sever, and R. A. DeBose-Boyd. 2005. Isolation of sterol-resistant Chinese hamster ovary cells with genetic deficiencies in both Insig-1 and Insig-2. *J. Biol. Chem.* **280:** 25242–25249.